IN-DEPTH INVESTIGATIONS OF PARAMETERS INFLUENCING THE ACCURACY OF ORTHOIMAGES FROM HIGH RESOLUTION SATELLITES

Henri Eisenbeiss[*], Emmanuel Baltsavias, Li Zhang[1]

Institute of Geodesy and Photogrammetry, ETH Zurich,

CH-8093, Zurich, Switzerland - (ehenri, manos)@geod.baug.ethz.ch, zhangl@casm.ae.cn

WG I/5 Geometric modeling of optical spaceborne sensors and DEM generation

KEY WORDS: Orthoimages, Accuracy analysis, High spatial resolution satellites

ABSTRACT:

Orthoimages are the most popular product from high spatial resolution satellite sensors. Various investigations, especially regarding Ikonos and Quickbird, have been published and achieved accuracies reported. However, these investigations are based on different input parameters (density and accuracy of DTM, number, distribution and accuracy of GCPs, sensor model, range of heights in the area, sensor elevation, type, amount and accuracy of information used to check the planimetric accuracy) and the published results are thus not comparable. Furthermore, the influence of the above mentioned parameters on the planimetric accuracy of the orthoimages has not been analysed using one common consistent dataset. In this work, we will try to cover this gap. In previous publications, we have presented a comparison of point positioning accuracies using various sensor models and different number and distribution of GCPs, so these aspects will not be treated in this work. Here, we have used in all cases as sensor model RPCs with a subsequent affine transformation and a small number of GCPs (8) with homogeneous distribution. The aspects that we analyse here is the influence of (a) the DTM, (b) the source and accuracy of GCPs, and (c) the sensor elevation.

1. INTRODUCTION

IKONOS imagery has been commercially available since early 2000. In recent years, a large amount of research has been devoted to the efficient utilization of these high spatial resolution images, and in particular regarding sensor modelling and image orientation (Baltsavias et al., 2001; Jacobsen, 2003; Grodecki and Dial, 2003; Fraser et al., 2002; Fraser and Yamakawa, 2003; Eisenbeiss et al., 2004a), automatic DSM/DTM generation (Jacobsen, 2004; Toutin, 2004; Zhang and Gruen, 2004; Poon et al., 2005; Toutin et al., 2004; Baltsavias et al., 2006), feature extraction (Lee et al., 2002; Tao and Hu, 2003; Di et al., 2001; Baltsavias et al., 2001 and 2004) and multi-channel color processing (Hong and Zhang, 2004; Ranchin and Wald, 2000).

In this paper, we will concentrate on the generation and accuracy analysis of mainly IKONOS and secondary Quickbird (QB) orthoimages. First evaluations of orthoimages from IKONOS Geo imagery are reported by Kersten et al. (2000), Toutin and Cheng (2000) and Davis and Wang (2001). Later work includes mapping using IKONOS images (Jacobsen, 2002) and the comparison of QB and IKONOS orthoimages (Jacobsen and Passini, 2003).

At IGP, first evaluations of IKONOS orthoimage accuracy were performed using suboptimal sensor models and/or GCP accuracy in object and/or image space (Kersten et al., 2000; Baltsavias et al., 2001; Vassilopoulou et al., 2002). The orthoimage accuracies achieved were mostly about 2m. Later studies using more accurate sensor models and better quality GCPs led to Ikonos and Quickbird orthoimage accuracies of 0.4-0.8 m (Eisenbeis et al., 2004a, 2004b).

The aim of this work is the analysis of orthoimage accuracy produced from IKONOS and QB images using different type of original data. More specifically, we are interested to see the influence of different sources for the measurement of GCPs (Ground Control Points), different elevation models and different sensor elevation on the planimetric accuracy. Although mathematical relations can establish the influence of sensor elevation and azimuth, and elevation and GCP errors on the planimetric accuracy of orthoimages, it is interesting to check with empirical tests what is the influence of various input data (especially DTMs/DSMs and GCPs), with known accuracy only globally.

The whole processing was performed mainly with Sat-PP (Satellite Imagery Precision Processing) software developed at IGP which makes use of good quality algorithms, especially for DSM generation and semi-automatic point measurement and feature extraction. The software can be used with any type of imagery, digital and scanned film, frame and linear sensors (ADS40 is currently under integration). In addition to Sat-PP, ArcGIS was used for manual measurement of GCPs, due to time constraints, easier handling of large datasets and support of various file formats.

2. DATA

2.1 Test areas

The test sites are shown in Fig. 1. The first area, Thun, lies in the central part of Switzerland 40 km southern of the capital of Switzerland, Bern. In this region in 2004, we established a testfield with a coverage of 15 by 20 sqkm for the analysis of high resolution satellite images. Later in 2006, this testfield was extended for the analysis of ALOS images to the neighborhood of Bern and Thun (30 by 30 sqkm).

In the area of Geneva we used IKONOS and QB images (Heller and Gut, 2004; Eisenbeiss et al., 2004b). The test area had a size of 16 by 17 km.

Both sites cover open, city, tree and alpine areas. The alpine areas in the northwestern and southeastern part of Geneva and in the southwestern part of Thun made it difficult to have a homogenous control point distribution.

---

[*] Corresponding author. http://www.photogrammetry.ethz.ch

[1] Now with the Institute for Photogrammetry and Remote Sensing, Chinese Academy of Surveying and Mapping, Bejing, P.R.China.
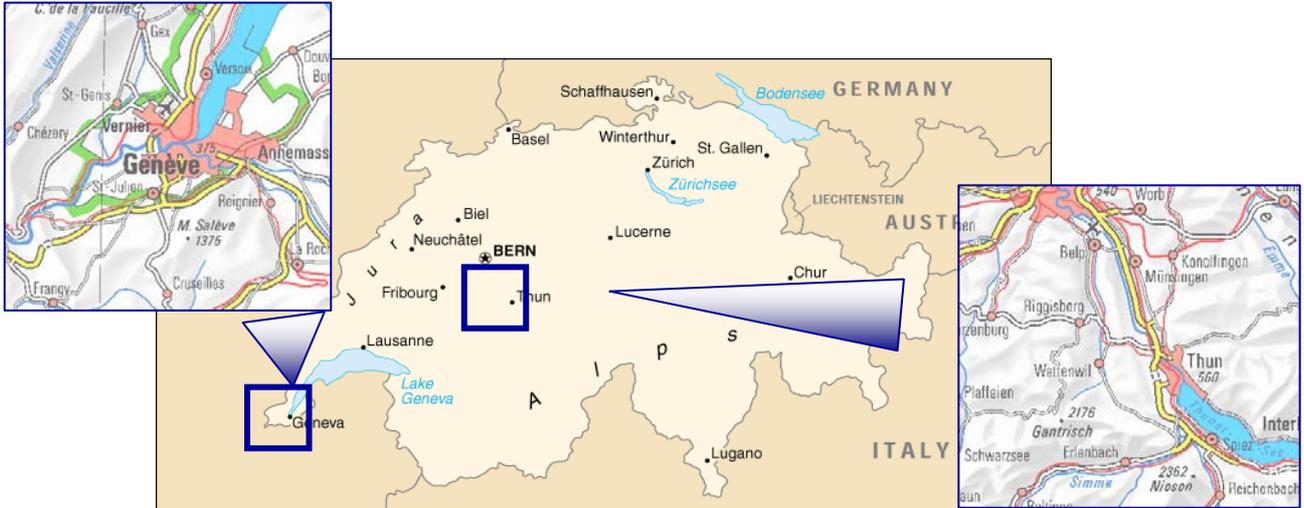
Figure 1. The test areas.

2.2 Satellite image data

In Geneva, we used two slightly overlapping IKONOS images (west and east, each about 10 km x 20 km) and one QB image covering the eastern and 60% of the western IKONOS images. In Thun, four Ikonos images (each covering an area of 10 km x 20 km) were used (see Table 1). The images taken in December and October had about 80% overlap. The December images were covered in about 70% of the area by snow and had long shadows, while the October images had almost now snow and better illumination conditions. Thus, usage of both October and December images could show to what extent the different image quality could have an effect on the orthoimage accuracy. The October images were generated with an interior orientation that had some errors, which influence mainly the y (flight) direction (see more details in Baltsavias et al., 2006). All IKONOS images were Geo, 11-bit with DRA off, with 1m panchromatic (PAN) and 4m multispectral (MS) channels, while the QB image was Basic 1B, 11-bit, 0.63m PAN and 2.52m MS. For the processing in both areas only PAN was used. The IKONOS and QB images had associated RPC files.

Image	Date of acquisition	Scanning mode	Sensor- Azimuth (deg)	Sensor-Elevation (deg)
Geneva_Q	2003-07-29	Reverse	286.4	77.6
Geneva_I_West	2001-05-28	Forward	253.6	67.2
Geneva_I_East	2001-05-28	Reverse	240.2	61.6
Thun_I_157928_001	2003-10-12	Forward	4.7	85.3
Thun_I_157928_002	2003-10-12	Reverse	197.1	71.95
Thun_I_163003_000	2003-12-25	Reverse	180.39	62.95
Thun_I_163003_100	2003-12-25	Reverse	72.206	82.13

Table 1. Specifications of used satellite images (Q stands for QUICKBIRD and I for IKONOS).

2.3 GCPs from GPS measurements

The GCPs in Thun were measured with differential GPS. GPS requires work in the field, but the accuracy obtained is higher (especially in height) and more homogeneous than using measurements in orthoimages, which have varying accuracy with unknown error distribution (due mainly to respective DSM/DTM errors).

The point distribution of the GCPs of Thun is shown in Fig. 2. 35 GCPs are available in the test area used in this paper. The GCPs were mainly intersections of road edges and their object coordinates had an accuracy of 0.2 -0.3 m. From the available 35 points, eight well defined and distributed points were selected for the image orientation.

2.4 GCPs from orthoimages

For both areas, the planimetric coordinates of GCPs were measured in orthoimages, while their height was interpolated from the respective DTM used in their generation.

For the measurement of GCPs in the Geneva site we used the Canton of Geneva orthoimages (OP-DIAE) (see Tab. 2). The GCP image coordinates in OP-DIAE were measured semi-automatically, see Section 3.1. The GCPs were road edge intersections but also quite some round-abouts. The point distribution of the GCPs in Geneva was homogeneous and can be found in Eisenbeiss et al. (2004b, Fig. 1). The number of GCPS in Geneva_I_East, Geneva_I_West and Geneva_Q was respectively: 34, 23 and 54.

In the Thun area, the national Swissimage orthoimages were used (see Table 2). The GCP image coordinates in Swissimage were measured manually. The GCPs were mostly road edge intersections. The GCP distribution was similar as the GPS points, and the same number of control were used.

The orthoimages from Geneva have a higher resolution and planimetric accuracy than Swissimage, therefore the GCPs there should be more accurate than those in Thun.
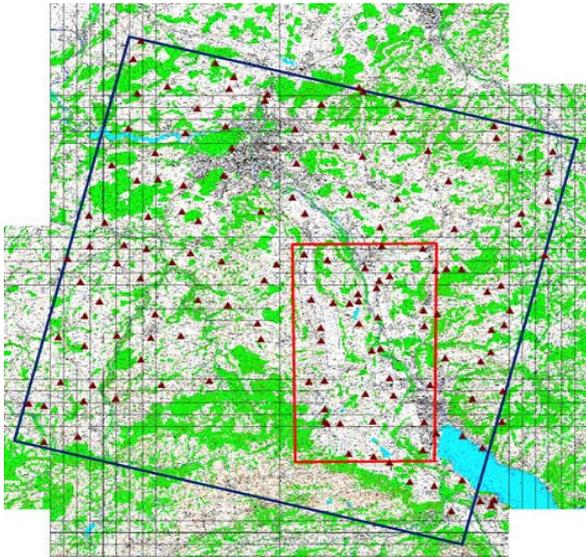

Figure 2. The GCPs (measured by GPS) distribution of our complete testfield in the area Thun/Bern are shown in the figure (outer rectangle). The control points covering the area

of the IKONOS images are displayed with the smaller rectangle. The figure shows the PK25 (Swisstopo ®).

2.5 Elevation data

In the area of Thun four different type of elevation data, laser DTM, DHM25, RIMINI and the elevation model produced by matching of the IKONOS images using Sat-PP, were used, while in Geneva a laser DTM and DHM25 were used. DHM25 and RIMINI cover the whole Switzerland, while the latter is free of charge. There are other national or world-wide DTMs of similar density and quality that are free or very cheap, thus it would be interesting to see what orthoimage accuracy could be achieved with RIMINI. In Table 2 the resolution and the accuracy of the elevation models are given. The matching DSM of Thun was produced using 3 images, had a grid spacing of 5 m and as compared to the laser DTM-AV its accuracy was 1-2 m in open areas, and about 3m in the whole area, excluding vegetation (for more details see Baltsavias et al., 2006). The matching algorithm of SAT-PP provides dense, precise and reliable results. It is explained in detail in Zhang, 2005 and Gruen et al. 2005.

All GCPs were on the ground, and thus there is no difference whether a DTM or DSM is used for orthoimage generation.

	OP-DIAE	DTM-AV	Swissimage	DTM-AV	DHM25	Rimini
Produced by	Canton Geneva		Swiss Federal Office of Topography (Swisstopo)			
Reference frame	LV03-GE	LV03-GE	LV03	LV03	LV03	LV03
Used elevation model	DTM-AV		DHM25			
GSD / grid spacing [m]	0.25	1.0	0.50	2.0	25.0	250
Planimetric accuracy [m]	0.50		1.0			
Accuracy of the height [m]		0.50		0.5/ vegetation: 1.5	Flat-hilly-Jura: 1.5 Voralps: 2 Alps: 5 - 8	average deviation to DHM25 is about 17

Table 2. Resolution and accuracy of used orthoimages and DTMs.

3. PROCESSING

3.1 Measurement of GCP image coordinates

In Geneva, some roundabouts and more straight line intersections (nearly orthogonal with at least 10 pixels length) were measured semi-automatically in the OP-DIAE orthoimages (see Fig. 3), using circle fit or line intersection with least squares, within Sat-PP. An unexpected complication was the fact that the Canton of Geneva is using an own coordinate system and not the Swiss one! The transformation from the Geneva to the Swiss system is not well defined, and based on different comparisons of transformed Geneva coordinates and respective coordinates in the Swiss system, a systematic bias has been observed, indicating that the results listed below could have been better. The measured GCPs in Geneva had an accuracy of 0.2-0.4 m.

In Thun, the same image measurement approach was used for the GPS points, however, roundabouts (which are better targets) were very scarce. As expected, well-defined points were difficult to find in rural and mountainous areas,

especially in the images taken in December, while shadows and snow made their selection even more difficult (Eisenbeiss et al., 2004a). The GCPs in Thun measured in Swissimage were measured manually in ArcGIS with an accuracy of 0.5-1 m. The GCPs in the October and December images were almost identical with some exceptions, due to the more difficult point identification in the December Ikonos images, especially the one with lower sensor elevation.
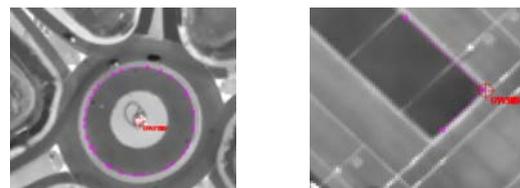

Figure 3. Examples of GCP measurement with circle fitting (left) and line intersection (right).

3.2 Preprocessing of the elevation models

The DTM-AV, DHM25 and Rimini in Thun were transformed from the CH1903 (Bessel_1841) coordinate system to the UTM(WGS84) zone 32 coordinate system. First, the height was transformed using a program of Swisstopo and then their planimetric position using ArcGIS. In Geneva the control points and the DTM-AV (LV03-GE) were transformed to the LV03 system using affine tranformation (6 Parameters). The heights were not corrected, since the used heights from LV95 are identical with the heights from LV03-GE see Heller and Gut (2004).

3.3 Sensor model and image orientation

In Eisenbeiss et al., 2004a, Gruen et al., 2005 and Baltsavias et al., 2006 we already analyzed the influence of several parameters like sensor model and number and distribution of control points on the image orientation. Our previous reserach showed that the sensor model using RPCs and a subsequent affine transformation is necessary for QB, while for Ikonos two shifts suffice for not very long images (see also Grodecki and Dial, 2003). For reasons of simplicity, here both Ikonos and QB images were oriented using first the RPCs to transform from object to image space and then using these values and the known pixel coordinates of GCPs to estimate the 6 affine parameters.

The results in Thun using 8 well distributed control points are listed in Table 3. The accuracy of the orientation using the GCPs measured with differential GPS is slightly better than with GCPs measured in Swissimage, especially in height due to the lower accuracy of DHM25. The orientation accuracy (RMS) for the Geneva images was in the range of 0.4-0.6 m (for more details see Eisenbeiss et al., 2004a).

Images	Type of GCP	GCP	CP	x-RMS [m]	y-RMS [m]	z-RMS [m]
2003-12-25	DGPS	8	27	0.37	0.40	0.56
2003-12-25	Orthoimage/DHM25	8	4	0.60	0.60	1.36
2003-10-12	DGPS	8	6	0.70	0.66	0.69
2003-10-12	Orthoimage/DHM25	8	7	0.74	0.90	0.98

Table 3. Results from the combined image orientation in Thun. CP are check points.

3.4 Orthoimage generation

For orthoimage generation, the panchromatic images were used to avoid possible additional errors from the pansharpening process. In Thun, the following orthoimage generation parameters were varied:
- 4 different DTMs/DSMs (Rimini, DHM25, DTM-AV, matching DSM)
- 2 GCP acquisition methods (GPS, from Swissimage orthoimages) and sensor orientations

- 2 sensor elevations (high, low)
- 2 epochs (December, October)

In Geneva, only the DTMs were varied (DHM25, DTM-AV).

The ground pixel size of the orthoimages was 1m for Ikonos and 0.7m for QB.

4. RESULTS AND ANALYSIS

The accuracy of the orthoimages was controlled by the use of check points. All check points were measured manually and not semi-automatically due to time constraints. Tables 4 and 5 below show the results for Thun and Geneva respectively. For Thun, only the results for the December images are shown, as the October images showed similar results and had smaller sensor elevation differences.

Orthoimage version	Number of CPs	Mean X (m)	Mean Y (m)	RMS X (m)	RMS Y (m)	Max Absolute X (m)	Max Absolute Y (m)
Rimini_GPS_DEC_63	20	0.01	-0.88	1.17	7.98	3.01	22.43
Rimini_ORTHO_DEC_63	20	0.10	-0.86	1.69	8.82	5.67	22.91
Rimini_GPS_DEC_83	**21**	**0.37**	**-1.20**	**1.04**	**2.06**	**2.29**	**3.62**
Rimini_ORTHO_DEC_83	21	0.30	-0.66	1.17	1.99	3.45	4.49
DHM25_GPS_DEC_63	20	0.09	-0.41	1.03	3.62	3.73	9.62
DHM25_ORTHO_DEC_63	20	-0.09	-0.31	1.04	3.69	2.35	10.23
DHM25_GPS_DEC_83	17	0.16	-0.86	0.92	1.34	2.20	3.17
DHM25_ORTHO_DEC_83	**19**	**0.10**	**-0.77**	**0.81**	**1.21**	**1.91**	**2.64**
Ma_GPS_DEC_63	20	0.23	-0.49	1.13	1.20	3.20	3.47
Ma_ORTHO_DEC_63	20	0.14	-0.38	1.29	1.14	3.98	2.94
Ma_GPS_DEC_83	**17**	**0.15**	**-0.67**	**0.72**	**0.95**	**1.72**	**1.89**
Ma_ORTHO_DEC_83	19	0.07	-0.43	0.72	1.02	1.85	2.31
LIDAR_GPS_DEC_63	12	-0.36	-0.18	1.03	0.95	2.60	2.04
LIDAR_ORTHO_DEC_63	11	-0.58	0.26	1.18	1.18	2.92	2.79
LIDAR_GPS_DEC_83	**11**	**0.29**	**-0.85**	**0.81**	**1.15**	**2.38**	**2.13**
LIDAR_ORTHO_DEC_83	10	-0.26	0.44	1.11	1.02	3.20	2.42

Table 4. Orthoimage accuracy in the Thun test area. The version with the lower RMS values for each DTM/DSM dataset are shown in bold.

Orthoimage version	Number of CPs	Mean X (m)	Mean Y (m)	RMS X (m)	RMS Y (m)	Max Absolute X (m)	Max Absolute Y (m)
I_West_ DTM-AV	10	0.1	0.0	0.5	1.0	0.8	1.9
I_West_DHM25	9	-0.4	0.0	1.0	1.1	1.9	1.8
I_East_ DTM-AV	11	0.2	-0.7	0.3	1.1	0.7	2.0
I_East_DHM25	11	0.0	-0.7	0.8	1.2	1.7	2.5
QB_DTM-AV	13	**0.2**	**-0.2**	**0.6**	**0.9**	**1.2**	**2.6**
QB_DHM25	13	0.2	-0.2	0.7	1.0	1.1	2.8

Table 5. Orthoimage accuracy in the Geneva test area.

4.1 Analysis of Thun results

The accuracy estimates, especially the RMS, are only slighter worse for GCPs coming from orthoimages compared to the GPS GCPs. This is mainly because the other error sources have a much more significant influence and partly mask small differences between these two versions. The effect of sensor elevation is significant, as shown by the max absolute and RMS errors, and it increases as the DTM/DSM accuracy deteriorates. Only for the DTM-AV the sensor elevation is almost irrelevant. Due to the sensor azimuths the 63 degree sensor elevation results are much worse in Y than in X, while for the 83 degree sensor elevation the Y results are only slightly worse than those in X. The influence of the sensor azimuth on the distribution of the height errors between X and Y increases as the accuracy of the DTM/DSM deteriorates. The effect of the DTM/DSM accuracy increases with decreasing sensor elevation. For 83 degree elevation, the matching DSM leads to slightly more accurate results than the DTM-AV, although it the first is less accurate than the later. The DHM25 provides regarding RMS similar results in X as the matching DSM and DTM-AV, however in Y the results in Y are worse, and also worse than the results Geneva (see below), maybe due to the rougher terrain in the Thun area. Some large mean Y values, e.g. for the LIDAR_GPS_DEC_83 version, are not explicable.

4.2 Analysis of Geneva results

The max absolute errors are in most cases higher in Y than in X, resulting in corresponding higher values for the RMS but curiously not always for the mean (see e.g. the QB results). The reason for the higher errors in Y should be mainly due to errors in the measurement of the image coordinates of the check points, since DTM errors, due to the sensor azimuth should influence X and Y almost equally. The RMS values for the 3 images is similar for the DTM-AV versions. The same applies to the DHM25 versions. This verifies previous conclusions that there is no significant accuracy difference between Ikonos and QB when the sensor model mentioned above is used, in spite of the higher spatial resolution of the later, and in this case also the higher sensor elevation.

There are no big differences between DTM-AV and DHM25. These exist only in X and only for the Ikonos images. Again due to the sensor azimuth DTM errors should influence X and Y almost equally, so the difference between X and Y should be attributed to errors in the measurement of the image coordinates of the check points.

The fact that the CPs were measured manually in the generated orthoimages may mask some differences among the various versions. This is also the reason why the accuracy values reported here are slightly worse than those reported in Eisenbeiss et al. (2004a), where the check points were measured semi-automatically.

In any case, the accuracies achieved by using the much cheaper DHM25, for typical (and suboptimal) sensor elevations, are in the 1m range, although the height accuracy of DHM25 is worse. This is due to the very narrow FOV of Ikonos and QB. The critical factor for achieving such accuracies, however, is the use of a proper sensor model, correcting the RPCs, and the accurate measurement in object and image space of the GCPs.

5. CONCLUSIONS

The results of this empirical test have verified the theoretical expectations. They are valid for the given Swiss input data, but we believe that in many other countries following similar geodata generation and quality control procedures as in Switzerland the results would be similar.

High accuracy DTM/DSM, as the DTM-AV and the matching DSM, provide more similar accuracy in X and Y, quite independently of the sensor azimuth and elevation. As the DTM/DSM accuracy deteriorates, a higher sensor elevation is needed and the height errors are distributed in X and Y differently, depending on sensor azimuth. For high sensor elevation (in this case 83 degrees), an orthoimage accuracy of 1-2.5 m was achieved even with the RIMINI dataset.

The major influence on the orthoimage accuracy is from the DTM/DSM and the sensor elevation. The role of GCP accuracy, as long as this is within certain limits (e.g. at least 1m) is subordinate. Since GCP acquisition is costly and time consuming, the selection of GCP acquisition method should be made based on the accuracy of the available DTM/DSM and the sensor elevation.

The current analysis could be better, if in all versions the same control and check points could have been used and measured with the same semi-automatic procedures in image space. However, we believe than this deficiency does not influence the main conclusions drawn here.

The use of a few CPs, which are generally on the ground and well-defined, does not permit a dense control of the orthoimage accuracy. Usage of high accuracy vector data, especially roads, and overlaying of them on the orthoimages, could help a lot for a visual control, but a quantitative evaluation would be difficult and rural and mountainous areas would have a sparser control. Another alternative would be to generate a very accurate reference orthoimage, and then compare other orthoimage versions by a dense matching between them and the reference one. In this case, matching would be easier due to the fairly

good approximations and would be also easier if all orthoimages are generated by either a DTM or DSM.

REFERENCES

Baltsavias, E. P., Pateraki, M., Zhang, L., 2001. Radiometric and Geometric Evaluation of IKONOS Geo Images and Their Use for 3D Building Modeling. Joint ISPRS Workshop on "High Resolution Mapping from Space 2001", Hannover, Germany, 19-21 September (on CD-ROM).

Baltsavias, E. P., L. O'Sullivan, C. Zhang, 2004. Automated Road Extraction and Updating using the ATOMI System – Performance Comparison between Aerial Film, ADS40, IKONOS and QuickBird Orthoimagery, International Archives of Photogrammetry and Remote Sensing, 35 (B4):1053-1058.

Baltsavias, E., Zhang, L., Eisenbeiss, H., 2006. DSM Generation and Interior Orientation Determination of IKONOS Images Using a Testfield in Switzerland. Photogrammetrie, Fernerkundung, Geoinformation, (1), pp. 41-54.

Davis, C.H., Wang, W., 2001. Planimetric accuracy of Ikonos 1-m panchromatic image products. Proc. ASPRS Annual Conference, St Louis, 23-27 April 2001, 14 p. (on CD-ROM).

Di, K., R. Ma, R. Li, 2001. Deriving 3-D Shorelines from High Resolution IKONOS Satellite Images with Rational Functions, Proceedings of ASPRS Annual Convention 2001, 25-27 April, St. Louis, Missouri (on CD-ROM).

Eisenbeiss, H., Baltsavias, E. P., Pateraki, M., Zhang, L., 2004a. Potential of IKONOS and QUICKBIRD Imagery for Accurate 3DPoint Positioning, Orthoimage and DSM Generation. IAPRS, Vol. 35 (B3): 522-528.

Eisenbeiss, H., Baltsavias, E., Pateraki, M., Zhang, L., Gut, O., Heller, O., 2004b. Das Potenzial von Ikonos- und Quickbird-Bildern fuer die genaue 3D-Punktbestimmung, Orthophoto- und DSM-Generierung. Geomatik Schweiz, (9), pp. 556-562.

Fraser, C., E. P. Baltsavias, A. Gruen, 2002. Processing of IKONOS Imagery for Sub-meter 3D Positioning and Building Extraction, ISPRS Journal of Photogrammetry & Remote Sensing, 56(3):177-194.

Fraser, C., Yamakawa, T., 2003. Applicability of the affine model for IKONOS image orientation over mountainous terrain. Joint ISPRS/ EARSeL Workshop on High-Resolution Mapping from Space 2003, Hannover, Germany, 6-8 October (on CD-ROM).

Grodecki, J., Dial, G., 2003. Block Adjustment of High-Resolution Satellite Images Described by Rational Polynomials. Photogrammetric Engineering and Remote Sensing, 69(1): 59-68.

Gruen, A., Zhnag, L., Eisenbeiss, H., 2005. 3D precision processing of high satellite imagery. ASPRS 2005 Annual Conference, Baltimore, Maryland, USA, March 7-11, on CD-ROM.

Heller, O., Gut, O., 2004. Auswertung hochauflösender Satellitenbildern IKONOS/QUICKBIRD, Internal Report, ETH Zurich, Switzerland.

Hong, G., Y. Zhang, 2004. The Effects of Different Types of Wavelets on Image Fusion, International Archives of Photogrammetric and Remote Sensing, 35 (B4):915-920.

Hu, X., C. V. Tao, 2003. Automatic Extraction of Main-Road Centerlines from IKONOS and Quick-Bird Imagery Using Perceptual Grouping, Proceedings of ASPRS Annual Convention 2003, 5-9 May, Anchorage, Alaska (on CD-ROM).

Jacobsen K., 2002. Mapping with IKONOS images, proceedings of 22nd EARSeL Symposium, Prague.

Jacobsen K., 2003. Geometric Potential of IKONOS- and QuickBird-Images. In: D. Fritsch (Ed.), Photogrammetric Week '03, pp. 101-110.

Jacobsen K., Passini R., 2003. Comparison of QuickBird and IKONOS for the Generation of Orthoimages, ASPRS annual convention, Anchorage 2003, 9 p, on CD-ROM .

Jacobsen K., 2004. DTM Generation by SPOT5 HRS, International Archives of Photogrammetry and Remote Sensing, 35(B1):439-444.

Kersten, Th., Baltsavias, E., Leiss, I., Schwarz, M, 2000. IKONOS-2 CARTERRA^{TM} Geo – Erste geometrische Genauigkeitsuntersuchungen in der Schweiz mit hochaufgelösten Satellitendaten, VPK, Nr. 8, August 2000, pp. 490 – 497.

Lee, D. S., J. Shan, J. S. Bethel, 2002. Class-Guided Building Extraction from IKONOS Imagery, Photogrammetric Engineering and Remote Sensing, 69(2): 143-150.

Poon, J., Fraser, C., Zhang, C., Zhang, L., Gruen, A., 2005. Quality Assessment of Digital Surface Models Generated from IKONOS Imagery. Photogrammetric Record, 20(110): 162-171.

Ranchin, T., L. Wald, 2000. Fusion of High Spatial and Spectral Resolution Images: The ARSIS Concept and its Implementation, Photogrammetric Engineering and Remote Sensing, 66(1):49-61.

Tao, C.V., Hu, Y., 2001. A Comprehensive Study of the Rational Function Model for Photogrammetric Processing. Photogrammetric Engineering and Remote Sensing, 66(12): 1477-1485.

Toutin, Th., 2004. Comparison of Stereo-Extracted DTM from Different High-Resolution Sensors: SPOT-5, EROS-A, IKONOS-II, and QuickBird. IEEE Transactions on Geoscience and Remote Sensing, 42(10): 2121-2129.

Toutin, Th. , Cheng, P., 2000. Demystification of IKONOS! EOM , 9(7), pp. 17-21.

Toutin, Th., P. Briand, R. Chenier, 2004. DTM Generation from SPOT5 HRS In-Track Stereo Images, International Archives of Photogrammetry and Remote Sensing, 35(B1): 416-420.

Vassilopoulou, S., Baltsavias, E., Dietrich, V., Hurni, L., Lagios, E., Parcharidis, I., Pateraki, M.,: 2002. Orthophoto generation using IKONOS imagery and high-resolution DEM: a case study on volcanic hazard monitoring of Nisyros Island (Greece).

Zhang, L., 2005. Automatic Digital Surface Model (DSM) Generation from Linear Array Images. Ph. D. Dissertation, Institute of Geodesy and Photogrammetry, ETH Zurich, Switzerland, Report No. 88.

Zhang, L., Gruen, A., 2004. Automatic DSM Generation from Linear Array Imagery Data. IAPRS, Vol. 35(B3): 128-133.